Evolutionary Bi-Objective Optimization of Soil Cutting by Bull-Dozer: A Real-World Application

Nada Barakat and Deepak Sharma
Department of Mechanical Engineering
Indian Institute of Technology Guwahati
Assam, India, Pin-781039
Email: {n.barakat, dsharma}@iitg.ernet.in

***Abstract*—Optimization is a procedure of finding an optimal solution from the feasible search space. In single-objective optimization, the solution gets improved iteratively based on the objective function value. But, most of the real-world problems involve more than one objective. In such situation, many solutions are optimal which are known as Pareto-optimal solutions. In this paper, we aim to solve one real-world optimization problem from the domain of construction equipment called as bull-dozer. We first formulate a bi-objective optimization problem with one constraint for soil cutting and pushing by the bull-dozer and then, solve it using genetic algorithm. We mainly target to perform the post-analysis of Pareto-optimal solutions which can evolve interesting relationships for the given problem.**

***Index Terms*—Bi-objective optimization; Post-optimal analysis, Soil Cutting and Pushing process; Soil-tool Interaction.**

I. Introduction

Optimization is a procedure for finding an optimization solution from the feasible search space which is constructed from the problem constraints and variable bounds. The optimization problems are generally solved for single-objective optimization. The optimization techniques developed for single-objective optimization improve the feasible solution iteratively by comparing the objective function value. Finally, a single optimal solution is generated. But, the real-world problems often involve many objectives that are to be achieved simultaneously [1]. Although there exists many classical methods for solving multi-objective optimization, but many of them are unable to generate non-convex Pareto-optimal front, discontinuous Pareto-optimal front etc. At the same, genetic algorithms (GAs) can solve multi-objective optimization problems in one run. It is because GA is a stochastic population based algorithm in which a population of solutions gets improved iteratively based on the concept of dominance which is stated that a solution $\mathbf{x}^{(1)}$ dominates $\mathbf{x}^{(2)}$ (denoted as $\mathbf{x}^{(1)} \prec \mathbf{x}^{(2)}$)

$$\begin{array}{ll} \forall i \in 1,2,\ldots,m: & f_i(\mathbf{x}^{(1)}) \ngeq f_i(\mathbf{x}^{(2)}) \\ \exists j \in 1,2,\ldots,m: & f_j(\mathbf{x}^{(1)}) < f_j(\mathbf{x}^{(2)}), \end{array} \quad (1)$$

where m is the number of objectives, f_i is the objective function value of $i-$th objective.

Many real-world problems involving multiple objectives are solved using GA in the literature [1]. The advantage is that GA evolves a set of Pareto-optimal solutions in a single run. These solutions can help designers and decision makers to choose a solution based on comparison and the post-optimal analysis [2]. In this paper, a real-world application has been chosen and a bi-objective optimization formulation is developed. We target finding optimal parameters for the soil cutting and pushing process by the bull-dozer.

As we know, the bull-dozer is a construction and road machinery which is mounted with a metallic blade in the front to cut and push the soil [3]. First, the edge of the bull-dozer blade penetrates the soil up to a certain depth and then, the bull-dozer starts cutting and pushing the soil. This is referred as soil-blade interaction in the domain literature [3]. During this interaction, the blade experience enormous resistance due to friction, cohesion and adhesion between the blade and soil, and the soil and ground. It means that the bull-dozer engine has to supply enough power to overcome this resistance. If we want to reduce power requirement from the bull-dozer for completing the task, then the resistance should be reduced. The resistance can be minimized by setting the optimal input parameters for the bull-dozer and its blade. In the literature, the resistance or draft force has been found either experimentally [4], [5] or by developing analytical models [6], [7], [8] and numerical models [9].

Various experimental studies have been accomplished for finding the resistance forces during the soil-blade interaction. However, no emphasis has been given on setting the optimal values of input parameters [10]. Moreover, finding the optimal set of input parameters experimentally may not be economic.

The existing analytical models can calculate the resistance forces during the soil-blade interaction with reasonable accuracy when compared with the experimental outcome. These models are developed based on the soil failure zone which is modeled as a soil wedge [6], [11]. The model is further developed for three-dimensional (3D) soil failure zone [7], [8]. The dynamic behavior has also been considered by including velocity [12], [13] and acceleration in the model [14]. A close observation suggests that the optimal study has not been done in the literature to choose or select a set of input parameters. However, these models can be used for finding the optimal set of input parameters.

The numerical studies have also been performed using finite element method or discrete element method. The finite element models are based on the concepts of soil mechanics and the failure zone by using various models like constitutive equations of soil failure [14], [15], [16], hypo-plastic constitutive

978-1-5090-5674-3/17/$31.00

model [17], [18], elasto-plastic constitutive model [19], to name a few. The discrete element method is developed by simulating motion of large number of small particles of soil [9]. These models are more accurate than analytical models. But, the numerical models are computationally expensive. Therefore, the optimization procedure demands high computational time to find the optimal set of input parameters for the given problem.

The models discussed above can calculate the draft force which is experienced by the bull-dozer blade. The optimal set of the input parameters can reduce the draft force so that the power requirement from the bull-dozer engine can be reduced. It is observed from the literature that reducing the depth of cut of the bull-dozer blade can reduce the draft force [8], [20]. But, reducing depth of cut can reduce the productivity of the cutting and pushing process. The productivity can be defined as the volume of soil cut by the blade in one pass. Therefore, we formulate the given application in two-objective problem so that the optimal set of input parameters can found. Following are the contributions of this paper:

1) A bi-objective optimization formulation is developed for soil cutting and pushing process so that an optimal set of parameters can be found that can reduce the draft force and but also increase the soil cut volume.
2) The post-optimal analysis is performed so that unique relationships among the objectives and parameters can be found which may not be discovered in the literature.

The paper is organized in five sections. Section II presents the bi-objective optimization formulation for the soil cutting and pushing process. Section III presents optimization algorithm for solving the bi-objective optimization problem. Section IV analyzes the results and observations are presented. The paper is concluded in section V with a note on future work.

II. Bi-Objective Optimization Formulation

The soil cutting and pushing process by the bull-dozer is formulated in two objectives. The problem is modeled using seven decision variables which are cutting depth (D), blade cutting angle (α), speed of the bull-dozer (v), blade width (B), blade height (H), blade curvature radius (R) and the blade curvature angle (θ). First three design variables represent the operational conditions for the bull-dozer and rest are dimensions of the bull-dozer blade. The problem formulation is given in (2).

The flywheel power of the bull-dozer is chosen as 227.438 KNm/s and total weight of the bull-dozer is considered as ($G_1 = 328.613$ KN). The formulation is developed for the flat terrain. A mid-stiffness clay soil is considered and its properties are given in Table I.

Here, γ_o is the cut soil density (kg/m^3), γ is the uncut soil density (kg/m^3), C_o is the cohesion of cut soil (N/m^2), C is the cohesion of uncut soil (N/m^2), δ is the soil-metal friction angle (radians), A_d is the soil adhesion factor (N/m^2), β is the angle that the rapture plane makes with horizontal (radians), φ_o is the angle of accumulation of cut soil (radians), and φ is the angle of internal friction of soil (radians).

$$
\begin{array}{ll}
\min & F \text{ (Cutting force)}, \\
\max & V \text{ (Blade capacity)}, \\
\text{subject to:} & \\
& P_R \geq 0, \\
& \text{(Power requirement of bull-dozer engine)} \\
\text{variable bounds:} & \\
& 5 \leq D \leq 50, \\
& 0.785 \leq \alpha \leq 1.309, \\
& 0.278 \leq v \leq 1.389, \\
& 300 \leq B \leq 500, \\
& 100 \leq H \leq 250, \\
& 90 \leq R \leq 150, \\
& 1.047 \leq \theta \leq 1.309.
\end{array} \tag{2}
$$

TABLE I
Soil parameters [21]

Soil type	γ_o	γ	C_o	C
Mid-Stiffness clay	640.74	1601.85	1019.715	2039.43
δ	A_d	β	φ_o	φ
21.6	0	23	30	27

A. Objective Functions

1) Soil Cutting Force: For calculating the draft or cutting force, an analytical model is adopted from [8]. Various forces considered in the analytical model are shown in Figs. 1 and 2. The assumptions of this model are stated in [8].

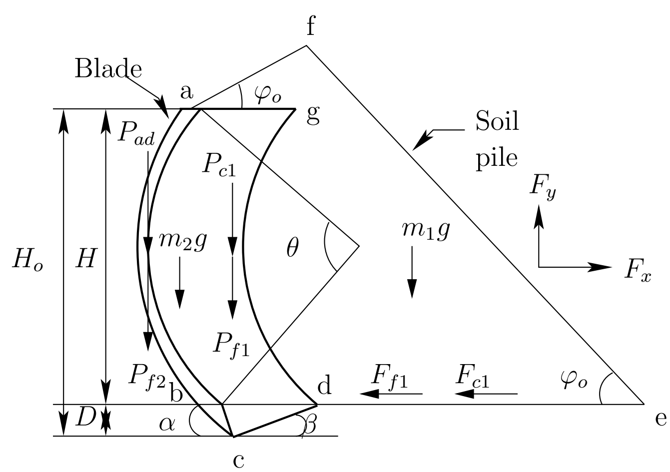

Fig. 1. Forces acting in the front of the blade [8].

The details of the forces are as follows,

1) The forces generated by the soil pile which is acting on the ground,
   - Weight of the soil pile on the ground is given as,

$$
m_1 g = (1/2)\gamma_o B(H + 2D\tan\varphi_o)^2 \cot\varphi_o \tag{3}
$$

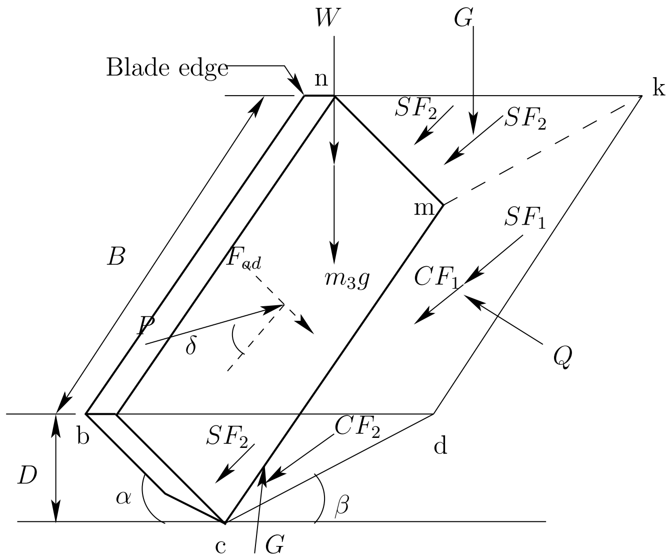

Fig. 2. Forces acting on a wedge of the soil in the front of the blade [8].

- Frictional force between the soil pile and the ground is given as,

$$F_{f1} = m_1 g \tan\varphi \tag{4}$$

- Cohesion force between the soil pile and the ground is given as,

$$F_{c1} = C_o B(H + 2D\tan\varphi_o)\cot\varphi_o \tag{5}$$

2) The forces generated by soil pile and the uncut soil,
   - Frictional force between the soil pile and the uncut soil is given as,

$$P_{f1} = (F_{f1} + F_{c1})\tan\varphi \tag{6}$$

   - Cohesion force between the soil pile and the uncut soil is given as,

$$P_{c1} = C_o BR\theta \tag{7}$$

3) The forces generated by the cut soil which is acting on the blade and its cutting edge as shown in Fig. 1,
   - Adhesion force between the cut soil and the blade is given as,

$$P_{ad} = A_{ad} BR\theta \tag{8}$$

   - Frictional force between the cut soil and the blade is given as,

$$P_{f_2} = (F_{f1} + F_{c1})\tan\delta \tag{9}$$

   - Weight of the cut soil sliding on the blade is given as,

$$m_2 g = 2\gamma_o BHD \tag{10}$$

4) The forces acting on the soil wedge which are shown in Fig. 2,
   - Weight of the soil wedge is calculated as,

$$m_3 g = (1/2)\gamma BD^2(\cot\alpha + \cot\beta) \tag{11}$$

   - Normal force acting on the interface between the blade and the soil wedge is calculated as,

$$G = (1/6)\gamma D^3(1 - \sin\varphi)(\cot\alpha + \cot\beta) \tag{12}$$

   - Frictional force acting on the interface between the blade and the soil wedge is calculated as,

$$SF_2 = G\tan\varphi \tag{13}$$

   - Cohesion force acting on the interface between the soil pile and the soil wedge is calculated as,

$$CF_2 = (1/2)CD^2(\cot\alpha + \cot\beta) \tag{14}$$

   - Normal force acting on the soil wedge is calculated as,

$$W = P_{f1} + P_{f2} + P_{ad} + P_{c1} + m_2 g + m_3 g \tag{15}$$

5) The forces occur in the soil rapture plane as shown in Fig. 2,
   - Cohesion force between the cut soil and the uncut soil is calculated as,

$$CF_1 = CBD/\sin\beta \tag{16}$$

   - Frictional force between the cut soil and the uncut soil is calculated as,

$$SF_1 = Q\tan\varphi, \tag{17}$$

   where Q is the normal force acting on the rapture plane.

6) The forces generated by the cut soil which is acting on the blade cutting edge,
   - Adhesion force between the soil and the cutting edge of the blade is given as,

$$F_{ad} = A_d BD/\sin\alpha \tag{18}$$

   - Force acting on the cutting edge of the blade is given as,

$$P = \frac{\begin{array}{c} W\sin(\beta+\varphi) - F_{ad}\cos(\alpha+\beta+\varphi) \\ +2SF_2\cos\varphi + 2CF_2\cos\varphi + CF_1\cos\varphi \end{array}}{\sin(\alpha+\beta+\varphi+\delta)} \tag{19}$$

The resultant forces acting on the blade are,

- The horizontal force is calculated as,

$$F_x = P\sin(\alpha+\delta) + F_{f1} + F_{c1} \tag{20}$$

- The vertical force (cutting force) is calculated as,

$$F_y = P\cos(\alpha+\delta) - (P_{f2} + P_{ad}) \tag{21}$$

The total resultant force is calculated as,

$$F = \sqrt{F_x^2 + F_y^2} \tag{22}$$

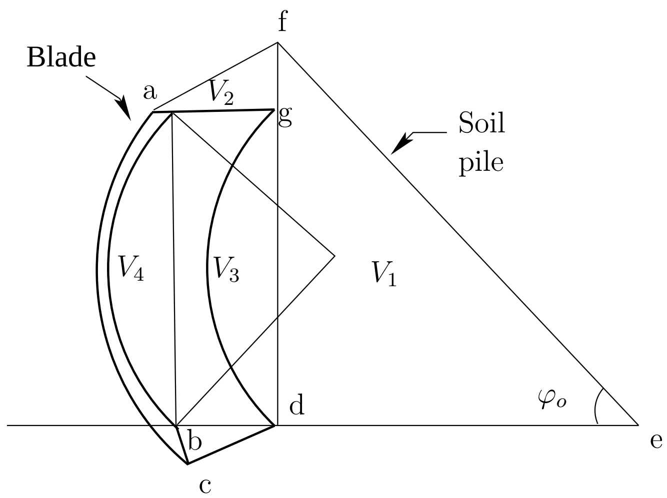

Fig. 3. Soil pile volume.

2) The Blade Capacity: In second objective function, the blade capacity is maximized which leads to maximizing the volume of cut soil in one cycle. In this paper, we assume that the blade is fully loaded with the soil and the blade capacity is equal to the volume of the soil pile accumulated in the front of the blade at the end of cutting and pushing process as shown in Fig. 3.

The blade capacity (V) is calculated as,

$$V = V_1 + V_2 + V_3 + V_4, \tag{23}$$

where,

- V_1 is the volume of (fde) which is calculated as,

$$V_1 = 0.5B(H + 2D\tan\varphi_o)^2 \left[\frac{1}{\tan\alpha}\right] \tag{24}$$

- V_2 is the volume of (afg) and it is calculated as,

$$V_2 = 2BD^2\tan\varphi_o \tag{25}$$

- V_3 is the volume of (abdg) that is calculated as,

$$V_3 = DHB\left[\frac{1}{\tan\alpha} + \frac{1}{\tan\beta}\right] \tag{26}$$

- V_4 is the volume of soil inside the arc (ab) and it is calculated as,

$$V_4 = 0.5B\theta R^2 - (0.5R^2 sin\theta) \tag{27}$$

3) Constraints: Only one constraint is designed for the given problem in which the bull-dozer can deliver sufficient power to overcome the resistance during cutting and pushing the soil. It is represented as P_R which is given as,

$$P_R = 0.85P_{bull} - P_w. \tag{28}$$

Here, P_{bull} is the flywheel power of the bull-dozer engine, and P_w is the required power at velocity v to overcome the resistance. In the literature, a quantity is defined as rim-pull, R_i, which is described as the force required from the bull-dozer engine to overcome the resistance offered by the cutting force (F) and the frictional force generated due to the weight of te bull-dozer. The rim-pull is given as,

$$R_i = F + \mu G_1. \tag{29}$$

Here, μ is the coefficient of frictional between the bull-dozer crawlers and the soil. P_w is thus calculated as $P_w = R_i v$.

III. Multi-Objective Genetic Algorithm

The bi-objective optimization formulated in the last section is solved using one of the benchmark multi-objective genetic algorithms known as elitist non-dominated sorting genetic algorithm (NSAG-II) [22]. From the literature, it is observed that NSGA-II has successfully solved different classes of problems arising in science and engineering domains [1]. It is a population based genetic algorithm which uses non-dominated sorting operator to find non-dominated solutions. Diversity among the solutions is maintained using crowding distance operator [22]. The NSGA-II algorithm is described using algorithm 1.

Algorithm 1 NSGA-II algorithm

```
Input: Population size (N), maximum generations (T), crossover probability, mutation probability, generation counter (t=0)
Output: Pareto-optimal solutions (P_{t+1})
Initialize random population P_t;
Evaluate P_t;
Assign rank using non-dominated sorting operator and diversity using crowding distance operator to P_t
while Generation counter t < T do
    P'_t := Selection(P_t) using crowded tournament selection operator;
    Q_t := Variation(P'_t) using simulated binary crossover operator and polynomial mutation operator;
    Evaluate Q_t;
    Merge population R_t = (P_t ∪ Q_t);
    Assign rank using non-dominated sorting operator and diversity using crowding distance operator to R_t;
    P_{t+1} := Choose best N solutions from R_t based on rank and crowding distance;
    t := t + 1;
end while
```

The NSGA-II algorithm initializes the population randomly. The population is then evaluated by calculating objective functions and constraint violation. The fitness is assigned to each solution of the population using non-dominated sorting and crowding distance operators. In a standard loop of NSGA-II, the crowded binary tournament selection operator is performed to select good solutions. The solutions are compared in a pair of two and the solution having better rank and larger crowding distance is selected over the other. The simulated binary crossover operator and polynomial mutation operator [23] are performed to generate the offspring population (Q_t). The parent population, P_t, and offspring population, Q_t, are merged to R_t, and non-dominated sorting and crowding distance are calculated for R_t. The best N solutions are chosen from R_t based on their better rank and larger crowding distance. This completes one generation of NSGA-II. The algorithm terminates when number of generations is equal to T.

IV. Results and Discussion

The bi-objective optimization of the given problem is solved using NSGA-II. The population size $N = 100$, maximum generation $T = 200$, crossover probability $p_c = 0.9$, mutation probability $p_m = 0.333$, crossover operator index $\eta_c = 15$ and mutation operator index $\eta_m = 20$ are kept fixed. As NSGA-II is a stochastic algorithm, we run it for 30 times with different initial population. Thereafter, the statistical analysis of results is performed by using inverse generalized distance indicator. This indicator is given as,

$$IGD = \frac{(\sum_{i=1}^{|P^*|} d_i^2)^{1/2}}{|P^*|}, \tag{30}$$

where P^* is the set of Pareto-optimal solutions, d_i is the Euclidean distance in the objective space between the solution $i \in P^*$ and the nearest member $k \in P_{t+1}$. The distance is calculated as,

$$d_i = \min_{k=1}^{|P_{t+1}|} \sqrt{\sum_{m=1}^{M} \left(\frac{f_m^{(i)} - f_m^{(k)}}{f_m^{max} - f_m^{min}} \right)^2}, \tag{31}$$

where m is the number of objectives, f_m^{max} and f_m^{min} are the maximum and minimum of $m-$th objective function values in P^*. It is noted that P^* is constructed by copying non-dominated solutions from the combined solutions of all 30 runs of NSGA-II.

The statistical values of IGD indicator are shown in Table II. Smaller statistical values of IGD indicator suggest that the performance of NSGA-II is consistent for solving the given problem.

TABLE II
The best, median and worst values of IGD indicator

Best value	Median value	Worst value
0.0267	0.0269	0.0269

The Pareto-optimal solutions of a NSGA-II run corresponding to the median IGD value are shown in Fig. 4. A clear trade-off between the two objectives can be observed. It suggests that a gain in one objective can lead to a loss in another objective. Although the mathematical equations of F and V appeared complex, but almost a linear relationship can be seen between the two objectives considered in this paper.

For better understanding of the results, the post-processing of the Pareto-optimal solutions is presented. In the literature [2], it is emphasized that the Pareto-optimal solutions should be analyzed for deeper understanding of the problem. Such analysis can discover interesting relationships and understanding to justify the specific pattern or commonality among the solutions.

We start our analysis by showing variation of cutting force for the cutting depth in Fig. 5. The figure shows that value of the cutting depth is evolved at its lower bound for generating

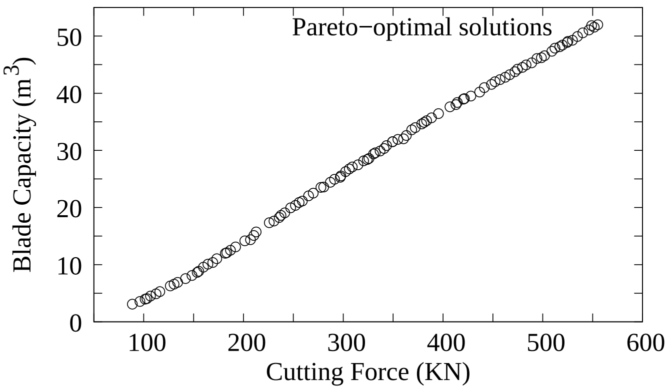

Fig. 4. The Pareto-optimal solutions generated by NSGA-II.

minimum force solutions. As the cutting depth increases and reaches to its upper bound, the cutting force also increases. Similar trend is also seen for V in Fig. 6 that minimum value of V is observed at the lower bound of the cutting depth. The volume of soil cut increases with increase in the cutting depth values. It is also justified from a linear relationship evolved between F and V showed in Fig. 4. The two transition zones are also seen in Figs. 5 and 6 which suggest that many Pareto-optimal solutions are converged to either lower or upper bound of D. Rest of the solutions shows increasing trend of cutting force and blade capacity with the cutting depth.

Next, we plot the second decision variable called as cutting blade angle (α) against the cutting force. As a linear trend can be seen between cutting force and blade capacity, plot for V against any decision variable are not shown in the paper. Fig. 7 shows that the cutting blade angle remains same for all Pareto-optimal solutions which is observed at its lower bound. This information is extremely important because it suggests to keep α at its lower bound for the optimal cutting and pushing of soil by the bull-dozer. The decision maker or operator of the bull-dozer can be benefited, if such information is available in-hand.

Another interesting relationship can be observed when cutting force is plotted against the width of the blade of the Pareto-optimal solution as shown in Fig. 8. It can be observed that many Pareto-optimal solutions are evolved at the lower bound of B. After the transition, F increases almost linearly with B for rest of the solutions.

In Fig. 9, an opposite relationship is observed when the cutting force is plotted against the height of the blade. Here, most of the Pareto-optimal solutions are evolved at the upper bound of H. For rest of the solutions which are very few, a linear trend can be seen which says that the cutting force increases with increase in H values.

Likewise the cutting angle of the blade, three more decision variables are evolved at their bounds for generating the Pareto-optimal solutions. Figs. 10, 11 and 12 show that R, θ and v are evolved at their lower bound. This information is handy and can be used effectively by the decision maker or operator to make the cutting and pushing process optimal.

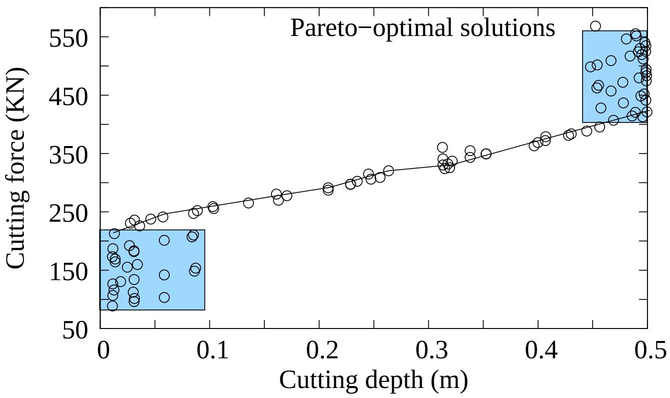

Fig. 5. The post-optimal relationship between the cutting force and the cutting depth.

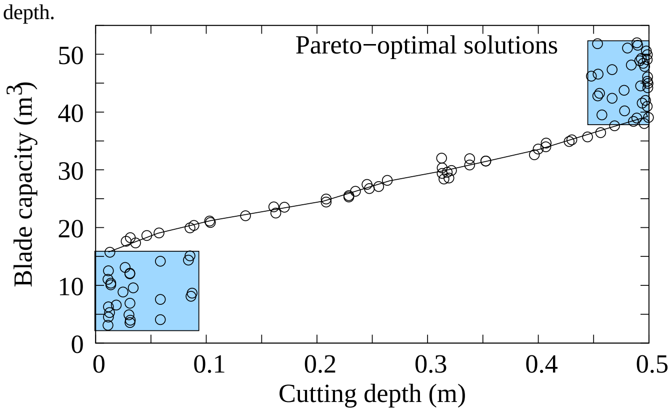

Fig. 6. The post-optimal relationship between the blade capacity and the cutting depth.

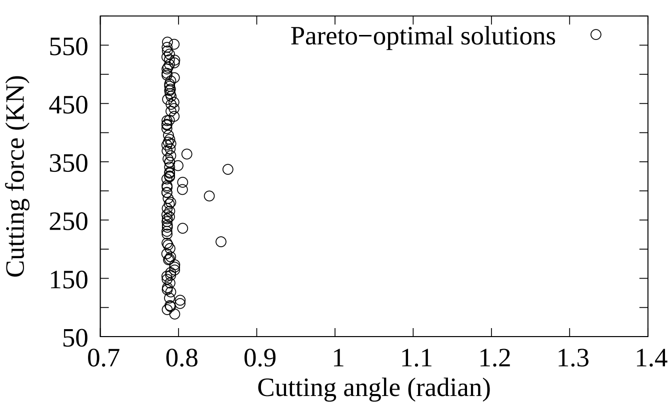

Fig. 7. The relationship between the cutting force and the blade cutting angle.

From the post-analysis of the Pareto-optimal solutions, it can be observed that α, R, θ and v should be kept at their lower bound for generating Pareto-optimal solutions for the given problem. Moreover, it can also suggested that D, B and H are important decision variables for evolving many Pareto-optimal solutions. As per the authors knowledge, such relationships are not available in the literature which we can only be found by solving the real-world problem with multiple objectives.

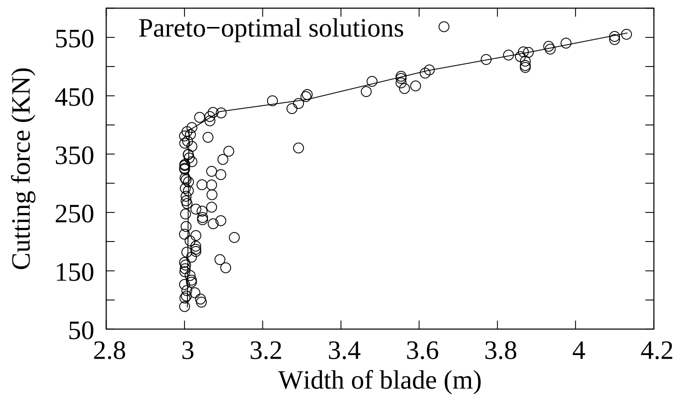

Fig. 8. The post-optimal relationship between the cutting force and the blade width.

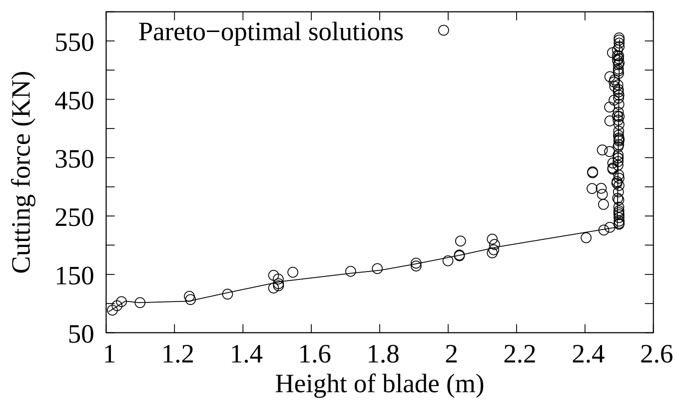

Fig. 9. The post-optimal relationship between the cutting force and the blade height.

The relationships have been discovered between the objective function and the decision variables. Now, we present the post-optimal analysis of the Pareto-optimal solutions by considering the decision variables only. Fig. IV shows the width of the blade is constant at its lower bound and the cutting depth increases for simultaneously minimizing the cutting force and maximizing the blade capacity. When the cutting depth reaches to its upper bound value, then width of the blade starts increasing for generating the Pareto-optimal solutions. In Fig. 13, the height of the blade first increases and reaches to its upper bound, then the cutting depth starts increasing. From both the figures, it can be observed that the Pareto-optimal solutions which are clustered at the lower bound of the cutting depth are generated due to increase in the height of the blade. When the height of the blade reaches to its upper bound, then the cutting depth increase. Finally, the cutting depth reaches to its upper bound value, then the width of the blade starts increasing. This information can be useful for the decision maker or operator to choose the right blade by focusing more on the height of the blade as compared to its width to increase the capacity of the blade which signifies volume of soil cut or productivity. The depth of cut is always a critical decision variable for minimizing the cutting force.

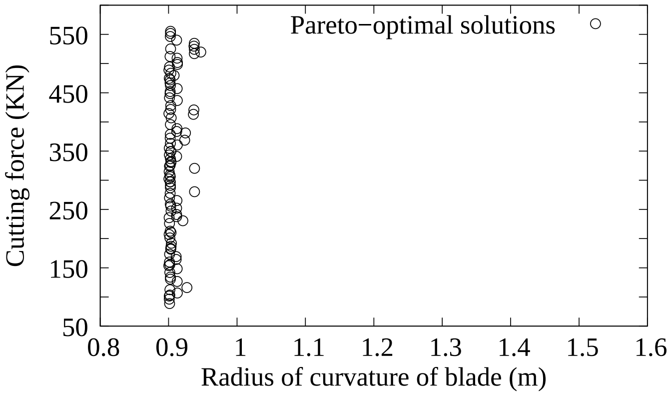

Fig. 10. The post-optimal relationship between the blade curvature radius and the objective functions.

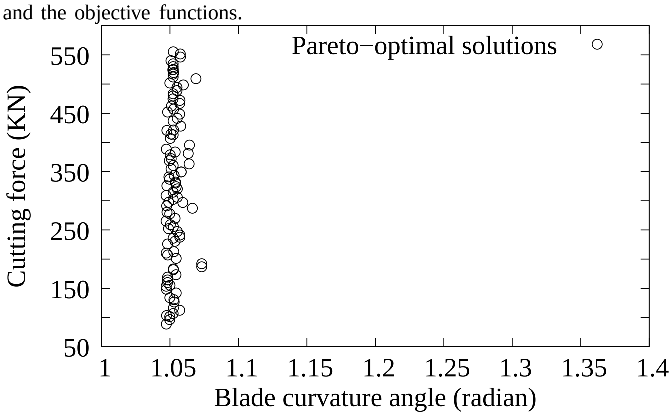

Fig. 11. The relationship between blade curvature angle and objective functions.

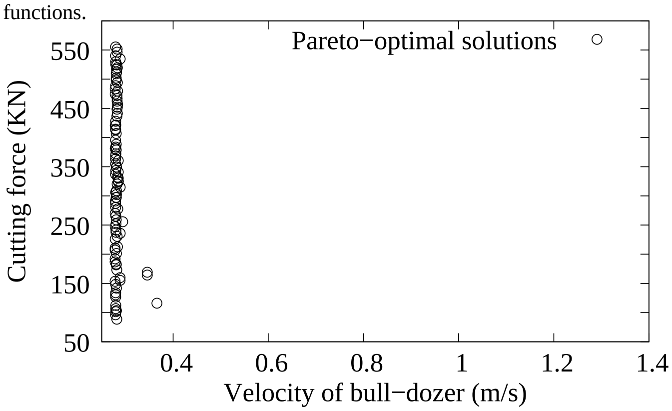

Fig. 12. The relationship between blade curvature angle and objective functions.

V. Conclusion

In this paper, a real-world problem of soil cutting and pushing by the bull-dozer was presented in terms of two objectives, seven decision variables and one constraint. The problem was solved using NSGA-II. The Pareto-optimal solutions generated from the study and their post-optimal analysis suggested the following conclusions:

- The two-objective developed in this paper showed a trade-off with almost a linear relationship between them.

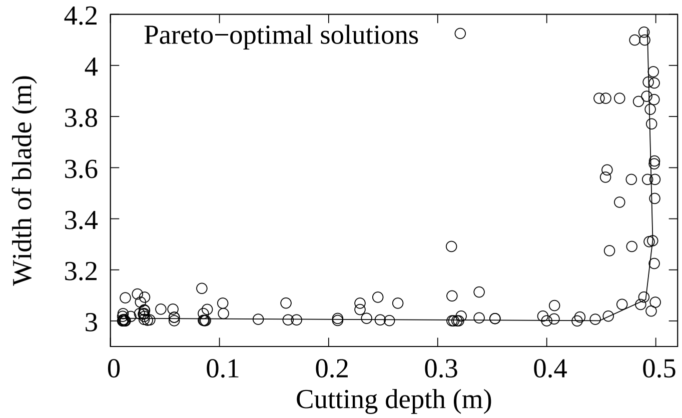

Fig. 13. The relationship between the cutting depth and the width of the bull-dozer blade.

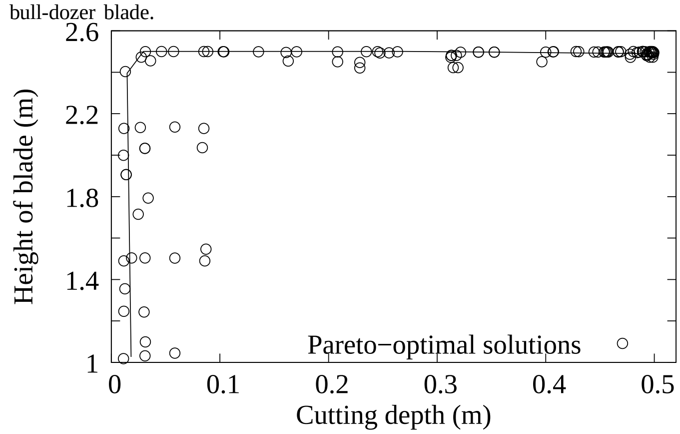

Fig. 14. The relationship between the cutting depth and the height of the bull-dozer blade.

- The cutting depth was an important decision variable for cutting and pushing the soil to make the process optimal. An increasing trend of F and V have been observed with increase in D.
- Similar to D, B and H also showed increasing trend for F. However, many Pareto-optimal solutions are evolved at the lower bound of B and at the upper bound of H.
- The decision variable α, R, θ and v were evolved at their lower bounds for generating the Pareto-optimal solutions.

In the future work, more realistic decision variables, objective functions and constraints can be included in the formulation. Other multi-objective algorithms can used for comparison.

Acknowledgment

First author of this paper extends her gratitude to Indian Council for Cultural Relations and acknowledges the support for her studies and research.

References

[1] K. Deb, *Multi-Objective Optimization using Evolutionary Algorithms*. Chichester, UK: Wiley, first ed., 2001.

[2] K. Deb and A. Srinivasan, “Innovization: Innovating design principles through optimization.,” in *Proceedings of the Genetic and Evolutionary Computation Conference (GECCO-2006)*, (New York: The Association of Computing Machinery (ACM)), pp. 1629–1636, 2006.

[3] R. L. Peurifoy, G. J. Schexnayder, and A. Shapira, *Construction Planning, Equipment and Methods*. McGraw-Hill Higher Education, 7 ed., 2006.

[4] D. Bagster and J. Bridgwater, “The measurement of the force needed to move blades through a bed of cohesionless granules,” *Powder Technology*, vol. 1, no. 4, pp. 189 – 198, 1967.

[5] K. Xia, “A framework for earthmoving blade/soil model development,” *Journal of Terramechanics*, vol. 45, no. 5, pp. 147 – 165, 2008.

[6] E. McKyes and O. S. Ali, “The cutting of soil by a narrow blade,” *Journal of Terramechanics*, vol. 14, no. 2, pp. 43–58, 1977.

[7] J. V. Perumpral, R. D. Grisso, and C. D. Desai, “A soil−tool model based on limited equilibrium analysis,” *Transactions of the American Society of Agriculture Engineers*, vol. 26, no. 4, pp. 991–995, 1983.

[8] Y. Qinsen and S. Shuren, “A soil-tool interaction model for bulldozer blades,” *Journal of Terramechanics*, vol. 31, no. 2, pp. 55 – 65, 1994.

[9] I. Shmulevich, Z. Asaf, and D. Rubinstein, “Interaction between soil and a wide cutting blade using the discrete element method,” *Soil and Tillage Research*, vol. 97, no. 1, pp. 37 – 50, 2007.

[10] A. Wislicki, “The influence of soil condition on the performance of a tracklayer operating a bulldozer,” *Journal of Terramechanics*, vol. 6, no. 2, pp. 35 – 45, 1969.

[11] D. Hettiaratchi and A. Reece, “Symmetrical three-dimensional soil failure,” *Journal of Terramechanics*, vol. 4, no. 3, pp. 45–67, 1967.

[12] W. Swick and J. Perumpral, “A model for predicting soil-tool interaction,” *Journal of Terramechanics*, vol. 25, no. 1, pp. 43 – 56, 1988.

[13] P. Gupta, C. Gupta, and K. Pandey, “An analytical model for predicting draft forces on convex-type wide cutting blades,” *Soil and Tillage Research*, vol. 14, no. 2, pp. 131 – 144, 1989.

[14] S. Karmakar and R. L. Kushwaha, “Dynamic modeling of soil-tool interaction: An overview from a fluid flow perspective,” *Journal of Terramechanics*, vol. 43, no. 4, pp. 411 – 425, 2006.

[15] M. Obermayr, K. Dressler, C. Vrettos, and P. Eberhard, “Prediction of draft forces in cohesionless soil with the discrete element method,” *Journal of Terramechanics*, vol. 48, no. 5, pp. 347 – 358, 2011.

[16] A. Armin, R. Fotouhi, and W. Szyszkowski, “On the {FE} modeling of soil-blade interaction in tillage operations,” *Finite Elements in Analysis and Design*, vol. 92, pp. 1 – 11, 2014.

[17] M. Abo-Elnor, R. Hamilton, and J. T. Boyle, “3d dynamic analysis of soil-tool interaction using the finite element method,” *Journal of Terramechanics*, vol. 40, no. 1, pp. 51 – 62, 2003.

[18] M. Abo-Elnor, R. Hamilton, and J. Boyle, “Simulation of soil-blade interaction for sandy soil using advanced 3d finite element analysis,” *Soil and Tillage Research*, vol. 75, no. 1, pp. 61 – 73, 2004.

[19] H. Bentaher, A. Ibrahmi, E. Hamza, M. Hbaieb, G. Kantchev, A. Maalej, and W. Arnold, “Finite element simulation of moldboard-soil interaction,” *Soil and Tillage Research*, vol. 134, no. 0, pp. 11 – 16, 2013.

[20] R. H. King, P. V. Susante, and M. A. Gefreh, “Analytical models and laboratory measurements of the soil−blade interaction force to push a narrow tool through JSC-1A lunar simulant and ottawa sand at different cutting depths,” *Journal of Terramechanics*, vol. 48, no. 1, pp. 85–95, 2011.

[21] A. S. D2487, “Standard practice for classification of soils for engineering purposes (unified soil classification system),” Tech. Rep. D2487, ASTM International, 2007.

[22] K. Deb, A. Pratap, S. Agarwal, and T. Meyarivan, “A fast and elitist multiobjective genetic algorithm: NSGA-II,” *Evolutionary Computation, IEEE Transactions on*, vol. 6, pp. 182 –197, apr 2002.

[23] K. Deb and R. B. Agrawal, “Simulated binary crossover for continuous search space,” *Complex Systems*, vol. 9, no. 2, pp. 115–148, 1995.